

# Simulation of a Ridge-type Semiconductor Laser with Selective Double-Sided Anti-guiding and Partially Undoped Cladding Layers

Daiya Katsuragawa and Takahiro Numai

Graduate School of Science and Engineering, Ritsumeikan University

1-1-1 Noji-Higashi, Kusatsu, Shiga 525-8577, Japan

Phone: +81-77-561-5161 E-mail: numai@se.ritsumeai.ac.jp

## 1. Introduction

High power 980-nm semiconductor lasers are very important as the light sources to pump erbium doped optical fiber amplifiers [1]. The cladding layers of 980-nm semiconductor lasers are AlGaAs layers. When buried structures are fabricated, AlGaAs layers are etched selectively before epitaxial regrowth to bury a mesa. Before the epitaxial regrowth, the surfaces of the etched AlGaAs layers are oxidized easily, and electrical and optical characteristics are highly degraded. To avoid these degradations, 980-nm semiconductor lasers have generally ridge structures to confine lateral modes. In the ridge structures, higher-order lateral modes as well as the fundamental lateral mode are confined. As a result, with an increase in injected current, higher-order lateral modes lase; kinks appear in their current versus light-output ( $I$ - $L$ ) curves [2]. The light output where a kink appears is called kink level. Below the kink level, only the fundamental lateral mode oscillates; above the kink level, higher order lateral modes oscillate. Light coupling efficiency to the single mode fiber of the higher-order lateral modes is much lower than that of the fundamental lateral mode. As a result, to obtain high fiber-coupled optical power, high kink levels or no kinks are required. To date, to increase the kink levels, coupling of the optical field to the lossy metal layers outside the ridge [3], highly resistive regions in both sides of ridge stripe [4], and incorporation of a graded V-shape layer [5] were investigated. To increase the kink level further, ridge structures with anti-guiding cladding layers [6], [7] have been proposed. In Ref. 7, kinks have not appeared, but the threshold current has been large due to lateral spreading of the injected current in the active layers below the anti-guiding cladding layers.

In this paper, a ridge-type semiconductor laser with selective double-sided anti-guiding and partially undoped cladding layers is proposed to reduce the threshold current. Since the undoped cladding layers have electrical resistance higher than p-doped cladding layers. As a result, lateral spreading of the injected current in the active layers below the anti-guiding cladding layers is suppressed, leading to low threshold current.

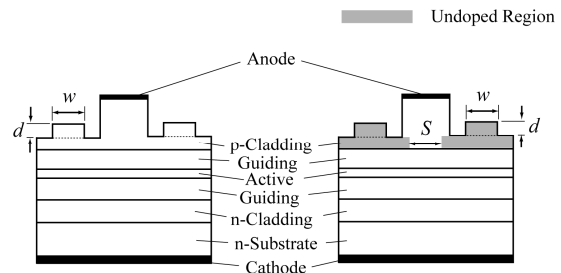


Fig. 1 Schematic cross-sectional view of (a) a ridge structure with selective double-sided anti-guiding cladding layers [7] and (b) a ridge-type semiconductor laser with selective double-sided anti-guiding and partially undoped cladding layers. The shaded areas are undoped.

## 2. Laser Structures and Simulations

Figure 1 shows a schematic cross-sectional view of (a) a ridge structure with selective double-sided anti-guiding cladding layers [7] and (b) a ridge-type semiconductor laser with selective double-sided anti-guiding and partially undoped cladding layers. The shaded areas are undoped. Here,  $S$  is the space between the undoped cladding layers;  $w$  is the width of the anti-guiding cladding layer;  $d$  is the thickness of the anti-guiding cladding layer. The distance between the top of the mesa and the top of the upper guiding layer is  $1.6 \mu\text{m}$  and the width of the mesa is  $3.3 \mu\text{m}$ . The base is  $60 \mu\text{m}$  wide, and the cavity is  $1200 \mu\text{m}$  long. Reflectivities of the front and rear facets are 2% and 90%, respectively.

Layer parameters such as band gap energy, refractive index, thickness, electron effective mass, hole effective mass, and doping concentration are the same as those described in Refs. 6 and 7. Lasing characteristics are simulated by using a device simulation software, ATLAS (Silvaco), which solves Poisson's equation and two-dimensional Helmholtz equation self consistently with a finite element method.

## 3. Simulation Results and Discussions

### 3.1 Size of the Anti-Guiding Cladding Layer

Figure 2 shows kink levels as a function the space  $S$  between the undoped cladding layers. The parameter is the width  $w$  of the anti-guiding cladding layer.

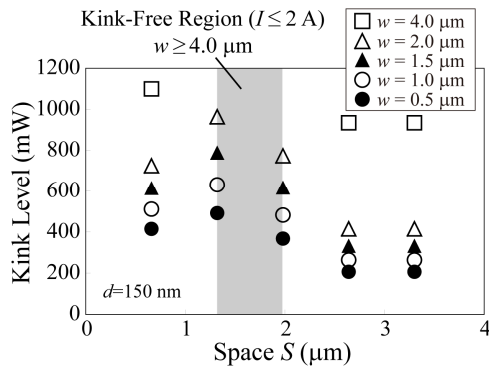


Fig.2 Kink levels as a function of the space  $S$  between the undoped cladding layers. Kink-free condition is  $w \geq 4.0 \mu\text{m}$  with  $1.32 \mu\text{m} \leq S \leq 1.98 \mu\text{m}$ .

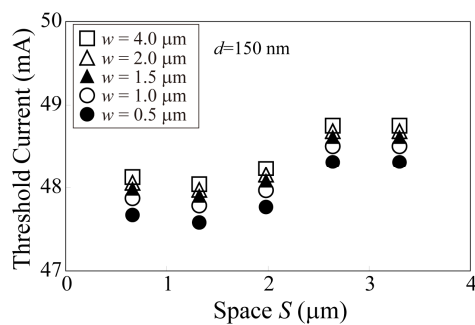


Fig.3 Threshold current  $I_{th}$  for the fundamental lateral mode as a function of the space  $S$  between the undoped cladding layers.

The minimum thickness of the p-cladding layer is 50 nm and the thickness  $d$  of the anti-guiding cladding layer is 150 nm. Kink-free region is indicated by a shaded area where the width  $w$  of the anti-guiding cladding layer is  $4.0 \mu\text{m}$  or more for  $1.32 \mu\text{m} \leq S \leq 1.98 \mu\text{m}$ . Figure 3 shows the threshold current  $I_{th}$  for the fundamental lateral mode as a function of the space  $S$  between the undoped cladding layers. The parameter is the width  $w$  of the anti-guiding cladding layer. The minimum thickness of the p-cladding layer is 50 nm and the thickness  $d$  of the anti-guiding cladding layer is 150 nm. At  $w=4.0 \mu\text{m}$  and  $S=1.32 \mu\text{m}$ , the lowest threshold current in the kink-free condition is obtained and its value is 48.0 mA, which is lower than the minimum threshold current of 57.0 mA in Ref. 7. With an increase in  $w$ , both of kink levels and threshold current increase.

### 3.2 Minimum Thickness of the p-Cladding Layer

Figure 4 shows kink levels as a function of the minimum thickness  $t$  of the p-cladding layer with  $d$  as a parameter for  $w=2.0 \mu\text{m}$ . Kink-free region, which is indicated by a shaded area, is obtained with an increase in  $t$ . Figure 5 shows the threshold current  $I_{th}$  for the fundamental lateral mode as a function of the minimum thickness  $t$  of the p-cladding layer for  $w=2.0 \mu\text{m}$  and  $d=50 \text{ nm}$ .

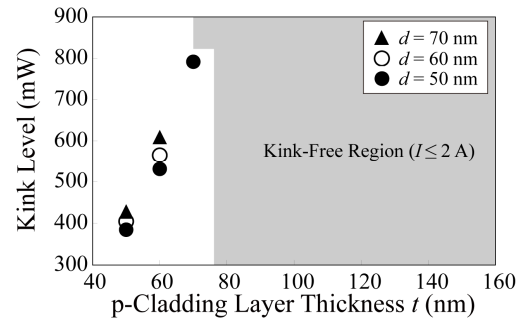


Fig.4 Kink levels as a function of the p-cladding layer thickness  $t$  with  $d$  as a parameter for  $w=2.0 \mu\text{m}$ .

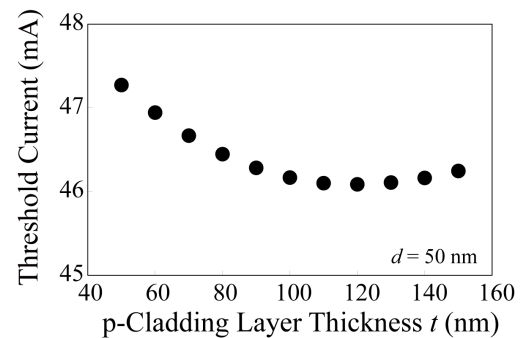


Fig.5 Threshold current  $I_{th}$  for the fundamental lateral mode as a function of the minimum thickness  $t$  of the p-cladding layer for  $w=2.0 \mu\text{m}$  and  $d=50 \text{ nm}$ .

In the kink-free condition, the lowest threshold current of 46.1 mA is obtained at  $t=120 \text{ nm}$ .

## 4. Conclusions

In a proposed ridge structure with selective double-sided anti-guiding and partially undoped cladding layers, the minimum threshold current was 46.1 mA, which is much lower than the minimum threshold current of 57.0 mA in Ref. 7.

## Acknowledgement

This research was partially supported by the Japan Society for Science, Grant-in-Aid for Scientific Research (C) 24560429, 2014.

## References

- [1] C. S. Harder et al., OFC'97, FC1, 1997, p.350.
- [2] M. F. C. Schemmann et al., *Appl. Phys. Lett.*, vol.66, pp.920-922 (1995).
- [3] M. Buda et al. *IEEE Photonics Technol. Lett.*, vol.15, pp.1686-1688 (2003).
- [4] M. Yuda et al., *IEEE J. Quantum Electron.*, vol.40, pp.1203-1207 (2004).
- [5] B. Qiu et al., *IEEE J. Quantum Electron.*, vol.41, p.1124-1130 (2005).
- [6] H. Takada and T. Numai, *IEEE J. Quantum Electron.*, vol.45, pp.917-922 (2009).
- [7] D. Katsuragawa and T. Numai, PIERS 2013 in Stockholm, Sweden (2013).